Modelling the morphodynamic effects of different design options for offshore sandpits

P.C. Roos[(1)] and S.J.M.H. Hulscher[(2)]

(1) & (2) Water Engineering and Management, Faculty of Engineering Technology, University of Twente, P.O. Box 217, 7500 AE Enschede, The Netherlands, p.c.roos@utwente.nl & s.j.m.h.hulscher@utwente.nl.

Abstract

We investigate the hydrodynamic and morphodynamic effects of sand extraction, for a variety of pit designs. To that end, we use an idealized model containing the essential physics for offshore bed evolution, based on the assumption that the ratio of pit depth to water depth is small. The resulting quasi-analytical tool enables a quick and extensive study into the effects of varying pit design parameters. The results show that sandpits, through the mechanism of flow contraction, trigger the morphodynamic instability behind sandbank formation (deepening, deformation, appearance of adjacent humps), and emphasize the influence of pit size, shape and orientation. The morphodynamic response is strongest for pits elongated in the preferred direction of sandbanks, and weakest for pits perpendicular to this direction.

1. Introduction

Shallow shelf seas, like the North Sea, are increasingly used as a source for sand (Hoogewoning and Boers 2001, Harrison 2003). However, large-scale sand extraction may have a negative impact on the hydrodynamics, morphology, coastal safety, ecology and biology of the system. This is of concern to the authorities responsible for issuing the permits for such projects. In this study, we restrict ourselves to the impact of large-scale sand extraction on the morphodynamics of the seabed, that is, to the effects on hydrodynamics, sediment transport and morphology.

The current legislation regarding sand extraction from the Dutch Continental Shelf prohibits mining landward of the 20 m depth contour, and defines a maximum pit depth of 2 m. Other practical constraints deal with the availability of sand, technical limitations and financial considerations. Besides, there are several degrees of freedom, related to the size and shape of the extraction area, as well as its orientation with respect to the flow. Suitable choices may minimize the potentially adverse impact.

Sand extraction can take place in two geometrically different ways: by creating sandpits, or by deepening existing navigation trenches. The morphodynamics of trenches have been studied by several researchers (Ribberink 1989, Walstra et al. 1998, Jensen et al. 1999ab, Van de Kreeke et al. 2002). Their model results show that trenches tend to migrate and deform gradually. Characteristic of the trench case, is its spatial uniformity in one horizontal direction, which simplifies the hydrodynamics of the problem, especially in the simplified case of perpendicular flow (Van de Kreeke et al., 2002).

The geometry of a sandpit is more complicated and may give rise to morphodynamic effects different from those in the trench case. For example, pits tend to display *flow contraction*, that is, the lateral attraction of water mass due to the reduced effect of bottom friction inside the pit (Ribberink 1989, Svašek 1998, Klein 1999, Hoogewoning and Boers 2001). The details depend on pit shape and orientation, but this influence has not been extensively studied. The flow conditions and horizontal dimensions (order km) of large-scale sandpits approximate those of tidal sandbanks, so also their morphodynamics may be related. This for example implies that the mechanism of tidal rectification (Zimmerman, 1981) may apply to sandpits. It describes the deflection of tidal flow as a result of friction-topography and Coriolis-topography interactions. Preliminary results (Roos et al. 2001, Roos and Hulscher 2003) indicate that creating a sandpit may trigger the corresponding instability related to sandbank formation (Huthnance 1982, De Vriend 1990, Hulscher et al. 1993). Currently, there is no detailed study into the hydrodynamics and morphodynamics of sandpits in relation to the degrees of freedom in pit design.

Our aim is therefore to develop a process-based morphodynamic model with the following properties. It should (i) contain the physics essential to offshore seabed evolution, including sandbank dynamics, (ii) be able to deal with a variety of *sandpit* geometries, and (iii) be sufficiently fast to allow an extensive sensitivity analysis regarding both pit design parameters and physical parameters. By legislation, the ratio of pit depth h_{pit} and water depth h_0 is small (except when extracting from shallow areas outside the 20 m depth contour, such as the crests of tidal sandbanks), which allows us to linearize with respect to the small parameter $e=h_{pit}/h_0$. Our focus will be on different aspects of the hydrodynamics (velocity and water levels inside pit, degree of flow contraction) and morphodynamics (evolution at pit center, migration). How do these indicators depend on the physics and on the pit design parameters?

Besides tidal sandbanks (wavelength ~ 5-10 km), the North Sea also displays the smaller-scale tidal sandwaves (wavelength ~ 100-500 m). Although the physical mechanisms forming these patterns are essentially different (Hulscher, 1996), both express an inherent instability of the seabed. The elements of pattern formation in the current analysis, aimed at *sandbank* dynamics, may therefore also be of help in understanding the relation between sand extraction and *sandwave*s.

The paper is organized as follows. In §2 we introduce the model, whereas the results are presented in §3. Finally, §4 and §5 contain the discussion and conclusions, respectively.

2. Model

2.1 Geometry

Consider an offshore part of a shallow shelf sea, in the absence of coastal boundaries, where we define a coordinate system with horizontal coordinates $\boldsymbol{x}=(x,y)$ (Figure 1). The z-axis points upward, with the free surface located at $z=?(\boldsymbol{x})$ and the seabed at $z=-h(\boldsymbol{x})$. We model a sandpit as a rectangular box of length L, width B and height h_{pit}, centered around the origin of the domain. The pit axis is inclined at an angle J with the direction the flow (the x-direction). The surrounding seabed is considered flat, at a uniform water depth h_0. Inside the pit, the water depth is h_0+h_{pit}, whereas the slopes at the edges of the pit follow a smooth, sinusoidal shape over a horizontal distance S. As characteristics of a sandpit we consider its length L, width B, orientation J and derived quantities such as its horizontal area BL (or its volume $h_{pit}BL$), and length-to-width ratio L/B. Note that, within our approach, the depth h_{pit} must be small with respect to the undisturbed water depth h_0. The averaged water flux across the line CD in Figure 1 (left) is a measure for the degree of flow contraction.

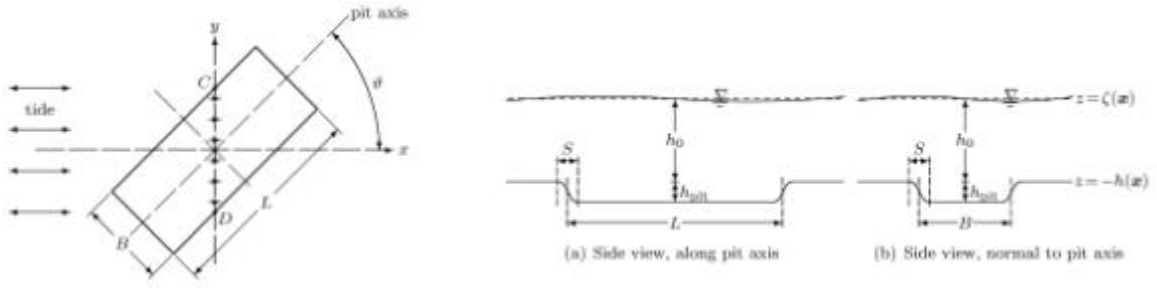

Figure 1: Sketch of pit geometry. Left: plan view, showing length L, width B, the pit axis as well as its orientation J with respect to the direction of the tidal flow. Right: side view, along (a) the length and (b) the width of the pit, showing the slope length S, the free surface level $z=?(\boldsymbol{x})$, the seabed $z=-h(\boldsymbol{x})$, the water depth h_0 and the pit depth h_{pit}.

2.2 Hydrodynamics

As the horizontal length scale (order km) is much larger than the vertical length scale (tens of metres), we follow a depth-averaged approach regarding the hydrodynamics. The shallow water equations read

$$g\ ??/?x + ?u/?t + u\ ?u/?x + v\ ?u/?y - fv + t_{bx}/h = 0, \quad (1)$$

$$g\ ??/?y + ?v/?t + u\ ?v/?x + v\ ?v/?y + fu + t_{by}/h = 0, \quad (2)$$

$$?(hu)/?x + ?(hv)/?y = 0, \tag{3}$$

where $\boldsymbol{u}=(u,v)$ is the depth-averaged flow velocity vector with components in x- and y-direction respectively. Moreover, g is the acceleration of gravity, t is time, and $f=2O\sin?$ a Coriolis parameter with $?$ the latitude and $O=7.292\cdot10^{-5}$ rad s^{-1} the angular frequency of the Earth's rotation. We have adopted the rigid-lid approach, implying that we neglect the contribution of $?$ to the local water depth. This is motivated by the small values of the Froude number $Fr=U(gh_0)^{-½}$, with U the maximum depth-averaged flow velocity during the tidal cycle (~ 1 m s^{-1}). Furthermore, bed evolution is so slow compared to the tidal cycle that a term $?h/?t$ does not need to be included in the continuity equation (3) (quasi-stationary approach). The bottom friction vector $t_b=(t_{bx},t_{by})$ is modelled linearly, according to $\boldsymbol{t}_b=C^{-2}g|\boldsymbol{u}|\boldsymbol{u}$, with C the Chézy parameter of nonlinear friction.

2.3 Sediment transport and bed evolution

The volumetric bedload sediment flux (in m^2 s^{-1}) is modelled as

$$\boldsymbol{q}_b = a_b(|\boldsymbol{u}|^2+½u_w^2)(u+ ?_b\tilde{N}h). \tag{4}$$

This is a third power law with coefficient a_b, including gravitational bedslope effects with coefficient $?_b$, and $\tilde{N}=(?/?x,?/?y)$. A wave stirring term $½u_w^2$ augments the amount of sediment transported by the tidal flow. We model the corresponding orbital velocity amplitude u_w as a negative power of the local water depth, that is, $u_w=U_w(h/h_0)^{-1}$, with amplitude U_w. The notion that the effect of wind waves is stronger in shallower water is incorporated in our stirring formulation.

The seabed evolves evolves on a *slow*, morphodynamic time $t=at$, which is well apart from the *fast* tidal time t. A detailed scaling procedure is not presented here (see, for example, Hulscher et al. 1993), and here we measure the slow time in units of years. Hence, only the *tidally averaged* sediment transport pattern matters. The seabed evolves as a result of tidally averaged divergences of bedload flux:

$$a^{-1}?h/?t = \tilde{N}\cdot\acute{a}\,\boldsymbol{q}_b\tilde{n}. \tag{5}$$

Here, the tidal average is defined as $\acute{a}\cdot\tilde{n}=T^{-1}\grave{o}\cdot dt$, integrating from $t=0$ to $t=T$ with T=12h25'. Finally, note that the bed porosity is included in the definition of the time coefficient a (~ $5.3\cdot10^{-8}$).

2.4 Flow conditions and solution procedure

First let us consider the situation *without* sandpit, that is, $h=h_0$ everywhere. Then, a spatially uniform flow of the form $\boldsymbol{u}_0=(u_0,v_0)=(j(t),0)$ with

$$j(t) = j_0 + j_2\cos st + j_4\cos(2st- f_4), \tag{6}$$

is a solution to the set of equations (1)-(5). This *basic flow* or *ambient flow* represents a bidirectional oscillatory tide with a residual component j_0, and semi-diurnal lunar component of amplitude j_2 angular frequency $s=1.41\cdot10^{-4}$ rad s^{-1} as well as its first overtide (amplitude j_4, phase lag f_4). The spatial uniformity of the flow makes it a *local* model, as we neglect the spatial variations on the lenght scale of a propagating tidal wave (wavelength ~ 700 km). The basic flow is then driven by an also spatially uniform, yet time-dependent pressure gradient $(\tilde{N}?)_0$. The associated sediment transport pattern is also spatially uniform, so the flat seabed remains flat. This holds for any choice of the wave stirring parameter U_w.

The idea is now to consider the situation *with* a pit as a small, local perturbation of this basic state, such that we may linearize in the parameter $e=h_{pit}/h_0$. To that end, we write $h=h_0+h_1$, $\boldsymbol{u}=\boldsymbol{u}_0+\boldsymbol{u}_1$, $\boldsymbol{q}_b=\boldsymbol{q}_{b0}+\boldsymbol{q}_{b1}$, where the subscript '1' refers to perturbed quantities, due to the presence of the pit. The resulting system for these first order quantities can be solved using a Fourier basis, which explains our spatially periodic approach on a square domain of about 50 x 50 km^2. Details of the solution procedure are not presented here due to lack of space, but they roughly follow existing literature (Huthnance 1982, De Vriend 1990, Hulscher et al. 1993). The model output consists of time-dependent flow and sediment

transport patterns, as well as the seabed topography, at arbitrary time t. Due to the local character of the sandpit, far away from the pit the basic or ambient conditions hold.

Table 1: Overview of model parameters (the four sets of tidal conditions I-IV will be referred to in §3).

.description	symbol				value(s)	dimension
latitude	?				52°N	deg
Coriolis parameter	f				$1.15\cdot10^{-4}$	s^{-1}
angular frequency of M_2-tide	s				$1.41\cdot10^{-4}$	rad s^{-1}
Chézy parameter	C				65	$m^{½}\ s^{-1}$
bedload transport coefficient	a_b				$4\cdot10^{-5}$	$m^{-1}\ s^{2}$
wave stirring velocity	U_w				0.25	m s^{-1}
water depth	h_0				20	m
pit depth	h_{pit}				2	m
pit length and pit width	L, B				1.0-15.0	km
slope length	S				0.2	km
orientation	J				-90°-90°	deg
Tidal conditions:		*I*	*II*	*III*	*IV*	
residual current	j_0	1.00	0.00	0.05	0.00	m s^{-1}
amplitude of horizontal M_2-tide	j_2	0.00	1.00	0.95	0.95	m s^{-1}
amplitude of horizontal M_4-tide	j_4	0.00	0.00	0.00	0.05	m s^{-1}
phase lag between M_2 and M_4-tide	f_4	0°	0°	0°	0°	deg

3. Results

3.1 General picture

First, for steady flow conditions (case I, see Table 1) and an obliquely oriented pit (L=3 km, B=2 km, J=30°) we investigate the main properties of the hydrodynamics (Figure 2). As a result of the reduced effect of the bottom friction inside the pit, the pit indeed displays flow contraction. This is witnessed by the velocity components, but also by the dipping of the free surface upstream of the pit. This dip provides the lateral pressure gradient, which attracts the flow toward the pit. As a measure for the degree of flow contraction we define the averaged added mass flux through the pit, according to

$$?Q_{pit} = (l_{CD}^{-1} \int_{CD} hu \, dy) - h_0 u_0 \qquad (7)$$

Here, we integrate across the line CD of length $l_{CD}=B\cos J$ (Figure 1). We also observe the generation of (positive and negative) vorticity over the edges of the pit, which is subsequently advected downstream. The depth-averaged vorticity, defined as $?=?v/?x-?u/?y$, is a measure for the degree of rotation and direction in the (depth-averaged) flow field. Vorticity production is strongest across the edges with a counterclockwise orientation; in these cases Coriolis and frictional effects amplify each other.

Now let us consider flow conditions more realistic for North Sea situations, consisting of an M_2-tide plus a small residual current (conditions III in Table 1). We now investigate the sediment transport pattern as well as the morphodynamic evolution of the pit (Figure 3). The pit dynamics display migration, deformation and the appearance of additional humps around the pit. The asymmetry in the forcing causes the pit to migrate, with a celerity up to several meters per year. Because of the deformation of the pit, migration requires a clear definition. Following Jensen et al.'s (1999b) treatment of the trench case, we define migration as the horizontal movement of the pit's center of 'mass':

$$\boldsymbol{c}_{mig} = ?\boldsymbol{x}_{CM}/?t, \qquad \boldsymbol{x}_{CM} = (BLh_{pit})^{-1} \int\int_D h_1(\boldsymbol{x},t)\,\boldsymbol{x}\, d\boldsymbol{x}, \qquad (8)$$

where we integrate of the full domain D. We will study this further in §3.3. Besides, the pit extends itself into a counterclockwise direction. Additional humps appear next to and downstream of the pit, thus indicating that a pattern of banks may gradually appear around the pit.

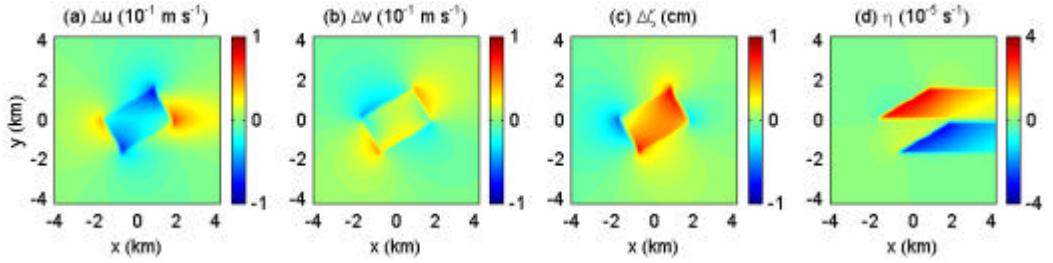

Figure 2: Hydrodynamics of sandpit with L=3 km, B=2 km, J=30°, subject to a steady flow from left to right. Plotted are the velocity components (a) $?u$, (b) $?v$, (c) the free surface response $??$ and (d) the vorticity field $?$. Parameter values taken from Table 1 (case I).

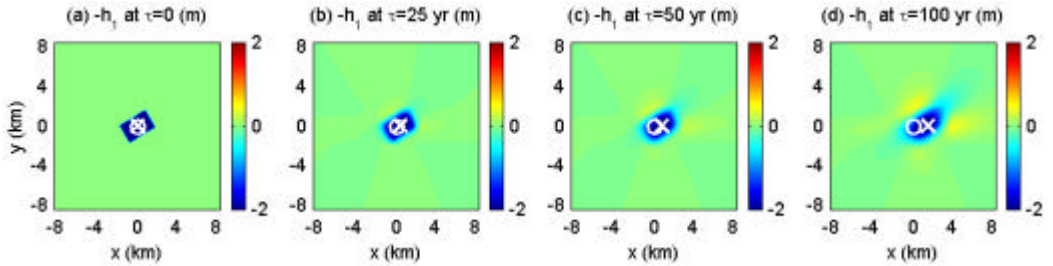

Figure 3: Evolution of sandpit with L=3 km, B=2 km, J=30°. Plotted are the topographies at (a) t=0, (b) t=25 yr, (c) t=50 yr and (d) t=100 yr. The origin is denoted with a circle, the pit's center of gravity with a cross. Parameter values taken from Table 1 (case III).

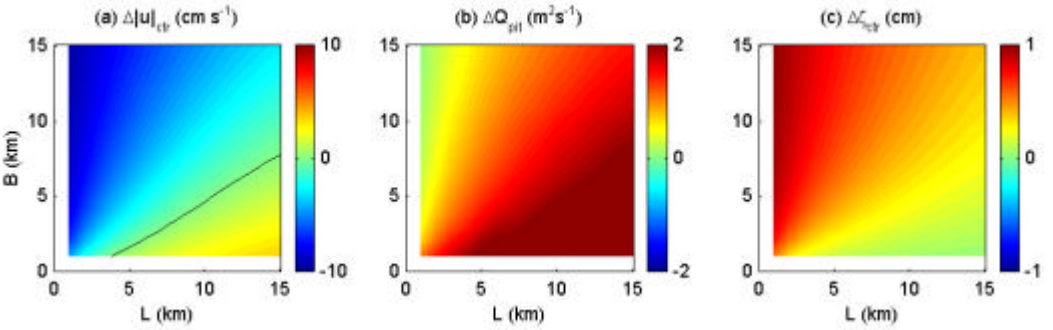

Figure 4: Hydrodynamics of steady flow over a sandpit with J=0°, as a function of pit length L and width B. Plotted are (a) $?U_{ctr}$, (b) $?Q_{pit}$, and (c) $?_{1,ctr}$. Parameter values taken from Table 1 (case I).

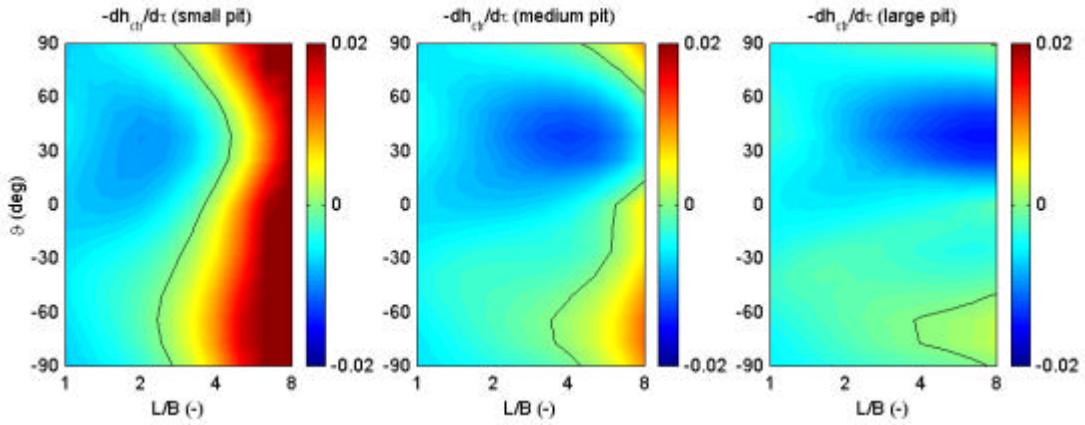

Figure 5: Bed evolution at pit center as a function of L/B and J : $?h/?t$ (in m yr^{-1}) at $\boldsymbol{x}$=**0** and t=0 for a pit of (a) small, (b) medium and (c) large size (8, 16 and 32 Mm^3, respectively). Parameter values taken from Table 1 (case II).

3.2 Sensitivity to pit design parameters

Now let us further investigate the dependence of this behaviour on the pit characteristics. Fixing the pit depth at h_{pit}=2 m and the water depth at h_0=20 m, we do this in two ways: considering (i) ranges of lengths L and widths B, for a fixed orientation, (ii) ranges of orientations J and length-to-width ratios L/B, for three different pit volumes: 8 Mm^3 (small), 16 Mm^3 (medium) and 32 Mm^3 (large).

First, we consider a steady current (case I), without oscillatory components. For a pit with its axis aligned with the flow J=0°, Figure 4 shows three hydrodynamic indicators: the velocity increase $?U_{ctr}=|u(0)|-j_0$ at the center of the pit, the added flux $?Q_{pit}$ as defined in equation (8), and the perturbed free surface elevation $??_{ctr}= ?_1(0)$ at the center of the pit. For pits elongated in the flow direction (large L/B) we find the highest values of $?U_{ctr}$. The longer the pit, the more space it allows for the flow to accelerate due to the reduced effect of bottom friction. For pits elongated in the direction normal to the flow (small L/B) we find $?U_{ctr}<0$, that is, pit velocities smaller than the basic flow. In this perpendicular trench-like case continuity governs the hydrodynamics, forcing the flow to slow down in deeper water.

In the case of a purely symmetrical tide (case II), the absence of migration allows us to study the evolution of the pit centre, by looking at the origin $\boldsymbol{x}=\boldsymbol{0}$. In general, smaller and wider pits tend to fill in, whereas larger and elongated pits erode at their centers (Figure 5). Moreover, there are specific orientations for which the response is strongest (J ~ 30°, that is, counterclockwise to current) and weakest (J ~ -60°). Finally, we note that the horizontal length of the pit slopes S hardly influences the results.

3.3 Migration

Having defined migration as the motion of the centre of gravity, one can show that the resulting migration rates depend on the flow conditions and not on the details of pit geometry:

$$\boldsymbol{c}_{mig} = a\acute{a}\boldsymbol{q}_{b0}\tilde{n}/h_0 \qquad (9)$$

(not derived here, for sake of brevity). Hence, migration takes place in the direction of the residual sediment transport. This simple result allows us to investigate the relation between migration and the various physical mechanisms, simply by looking at the properties of the basic state. As can be expected, the degree of tidal asymmetry, that is the effects of residual currents and M_4-components has an increasing effect on the migration rate (Figure 6a-c). In addition, stronger wave activity leads to higher migration rates, but this requires the presence of a residual current j_0 (Figure 6d).

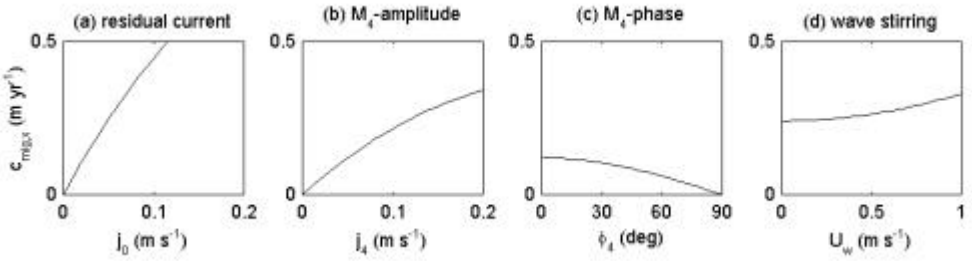

Figure 6: Dependency of migration celerity on (a) strength of the residual current (case III), (b) amplitude of the M_4-component (case IV), (c) phase of the M_4-component (case IV) and (d) wave activity (case III). The sum of amplitudes has been kept constant: $j_0+j_2+j_4$=1 m s^{-1}.

4. Discussion

The linearity in the bed amplitude makes the simulations quick, yet limits the applicability of this model to extraction areas with a small ratio of pit depth to water depth. Furthermore, the influence of pit depth can not be studied with this model. A nonlinear extension of the model could resolve this. However, such a strongly nonlinear two-dimensional horizontal approach, fully resolving the tidal components on a large-scale two-dimensional domain, will be computationally very expensive. Nevertheless, in view of the

recent changes in Dutch legislation towards permitting larger pit depths, this topic deserves further investigation.

Analogous to earlier research (Ribberink 1989, Svašek 1998, Klein 1999), we have modelled a sandpit as a disturbance of an otherwise flat seabed. The same type of offshore morphodynamic models has been used to show that the flat seabed is inherently unstable, giving rise to the formation of tidal sandbanks (Huthnance 1982, De Vriend 1990, Hulscher et al. 1993). These theories describe the formation of patterns of infinite spatial extent. In our results, the instability is triggered *locally* by the sandpit (Figure 4). Hence, the morphodynamic results comprise both the direct response to a pit, as well as the inherent instability of the flat seabed. Alternatively, we conclude that this instability is the morphodynamic manifestation of *flow contraction*.

Closely related to the properties mentioned above (linearity, flat seabed) is the issue of extracting sand from tidal sandbanks. Recently, the Zeeland Banks have been targeted as a potential source of sand on the Dutch Continental Shelf. The morphodynamic processes maintaining these features may interact with the sandpit. De Swart and Calvete (2003) have shown that, in the context of shoreface-connected sand ridges, the resulting behaviour can be essentially different from the results obtained for a flat bed. Note that the nonlinear study by Roos et al. (2004) provides the theoretical framework for such a study in the context of tidal sandbanks.

The physics of the model could be extended, for example by including suspended load transport. The spatial relaxation of suspended matter introduces an additional length scale, which may be important in relation to the pit dimensions. It could also be worthwhile to compare the effects of the nonlinear friction law adopted with a simpler linear parametrization. Finally, it is worthwhile to assess how to validate against field data. Recently, a 6.5 Mm^3 sample pit has been created off the Dutch Coast near Hook of Holland (L=1.3 km, B=0.5 km, h_0=24 m, h_{pit}=10 m). Several factors complicate the comparison with the model developed here: (i) the relatively large depth of the pit (h_{pit}/h_0=0.42), (ii) the site-specific stratification caused by the outflow of the Rhine, (iii) the absence of measurements in the upper part of the water column, and (iv) the relatively short monitoring period (half a year). For a comparison between the PUTMOR experiments and a process-based numerical code (DELFT-3D, both in a two-dimensional depth-averaged in a and three-dimensional setting), we refer to Walstra et al. (2002).

5. Conclusions

We have developed a process-based morphodynamic model for sandpit evolution, including the essential physics for large-scale offshore sea bed dynamics, as used in earlier studies. It allows an extensive sensitivity analysis with respect to the degrees of freedom in pit design, such as length, width, and orientation. The results have shown that a pit tends to display flow contraction, and that, as a morphodynamic implication of this hydrodynamic mechanism, it deforms, deepens, migrates, and creates adjacent humps. This morphodynamic response is strongest for elongated pits, with their length axis slightly counterclockwise to the direction of the tidal forcing. This is the preferred direction for the formation of tidal sandbanks, which emphasizes the link between between the morphodynamics of offshore bed features and large-scale sandpits. Alternatively, the response can be minimized when the main pit axis is oriented perpendicular to this preferred direction. Migration rates turn out to be controlled by the flow conditions (tidal components, wave activity) and not by pit geometry.

The main restrictive properties of this model are its linearity in the bed amplitude, and the starting with a flat seabed. An extension of the model into the (strongly) nonlinear regime, though computationally expensive and therefore not suitable for a sensitivity analysis, could improve these aspects. Especially the nonlinear response from tidal sandbanks to interventions is worthwhile to be investigated in the future.

Acknowledgment

This work has been carried out within the framework of the EU-project HUMOR, contract number EVK3-CT-2000-00037. We thank Attila Németh for his comments on an earlier version of this manuscript.

References

De Swart, H.E. and D. Calvete, Nonlinear response of shoreface-connected sand ridges to interventions, Ocean Dyn. 53(3), 270-277, 2003.

De Vriend, H.J., Morphological processes in shallow seas, *in* R.T. Cheng (ed.), *Residual currents and long-term transport, Coastal and estuarine studies,* Vol. 38, Springer-Verlag, New York, pp. 276-301, 1990.

Harrison, D.J., European overview of marine sand and gravel, *EMSAGG Conference 2003,* Delft, The Netherlands, 2003.

Hoogewoning, S.E. and M. Boers, Fysische effecten van zeezandwinning, *Technical Report RIKZ-2001.050,* RIKZ, Den Haag, The Netherlands, in Dutch, 2001.

Hulscher, S.J.M.H., H.E. De Swart, and H.J. De Vriend, The generation of offshore tidal sand banks and sand waves, *Cont. Shelf Res.* 13(11), 1183-1204, 1993.

Hulscher, S.J.M.H., Tidal induced large-scale regular bed form patterns in a three-dimensional shallow water model, *J. Geophys. Res.* 101(C3), 20,727-20,744, 1996.

Huthnance, J.M., On one mechanism forming linear sand banks, *Est. Coast. Shelf. Sc.* 14, 74-99, 1982.

Jensen, J.H., E.O. Madsen and J. Fredsøe, Oblique flow over dredged channels. I: flow description, J. Hydr. Eng. 125, 1183-1189, 1999a.

Jensen, J.H., E.O. Madsen and J. Fredsøe, Oblique flow over dredged channels. II: sediment transport and morphology, J. Hydr. Eng. 125, 1183-1189, 1999b.

Klein, M., *Large-scale sandpits,* Master's thesis, Civil Engineering, Delft University, Delft, The Netherlands, 1999.

Ribberink, J.S., Zeezandwinning. *Technical Report H825,* WL|Delft Hydraulics, Delft, The Netherlands, in Dutch, 1989.

Roos, P.C. and S.J.M.H. Hulscher, Large-scale sea bed dynamics in offshore morphology. Modeling human intervention, Rev. Geophys. 41(2), 1010, doi:10.1029/2002RG000120, 2003.

Roos, P.C., S.J.M.H. Hulscher, M.A.F. Knaapen and R.M.J. van Damme, The cross-sectional shape of tidal sandbanks: modeling and observations, *submitted to J. Geophys. Res,* 2004.

Roos, P.C., S.J.M.H. Hulscher, B.G.T.M. Peters and A.A. Németh, A simple morphodynamic model for sand banks and large-scale sandpits subject to asymmetrical tides, *in* S. Ikeda (ed.), Proc. RCEM Symposium, IAHR, Obihiro, Japan, pp. 91-100, 2001.

Svašek, Waterbeweging in zandwingebieden t.b.v. productK2000*z.w., *Technical Report 98454/1081,* Svasek b.v., in Dutch, 1998.

Van de Kreeke, J., S.E. Hoogewoning and M. Verlaan, An analytical model for the morphodynamics of a trench in the presence of tidal currents, Cont. Shelf Res. 22, 1811-1820, 2002.

Walstra, D.J.R., L.C. Van Rijn and S. Aarninkhof, Sand transport at the middle and lower shoreface of the Dutch coast; simulations of SUTRENCH-model and proposal for large-scale laboratory tests, *Technical Report Z2378,* WL|Delft Hydraulics, Delft, The Netherlands, 1998.

Walstra, D.J.R., L.C. Van Rijn and M.A.G. Van Helvert, Morphology of pits, channels and trenches. Part III: Investigation of the longshore and cross-shore impact of various pit designs, *Technical Report Z3223.30,* WL|Delft Hydraulics, Delft, The Netherlands, 2002.

Zimmerman, J.T.F. Dynamics, diffusion and geomorphological significance of tidal residual eddies, *Nature* 290, 549-555, 1981.